

TECHNICAL ARTICLE

Effective Degassing for Reduced Variability in High-Pressure Die Casting Performance

EWAN LORDAN ^{1,2} JAIME LAZARO-NEBREDA,^{1,3} YIJIE ZHANG,^{1,4}
and ZHONGYUN FAN^{1,5}

1.—Brunel Centre for Advanced Solidification Technology (BCAST), Brunel University, Uxbridge, Middlesex UB83PH, UK. 2.—e-mail: ewan.lordan@brunel.ac.uk. 3.—e-mail: jaime.lazaronebrea@brunel.ac.uk. 4.—e-mail: yijie.zhang@brunel.ac.uk. 5.—e-mail: zhongyun.fan@brunel.ac.uk

The reduced solubility of hydrogen in molten aluminium is believed to be a key factor influencing the formation of gas porosity, which adversely affects the mechanical properties. In this study, two crucibles of AlSi10MnMg alloy were degassed using conventional rotary degassing and high shear melt conditioning (HSMC) respectively and then cast into tensile specimens using the high-pressure die casting (HPDC) process. An optimal holding time of 10 min was established for both processing techniques corresponding to reduced density index (DI) and reduced variation in tensile performance. After rotary degassing, DI values were found to increase with increasing holding times, rising to 4.1% after 70 min. For HSMC, a quasi-steady state was observed with a maximum DI value of 1.4% after 190 min. The pore size in HPDC cast specimens was observed to be considerably lower after degassing with the HSMC device compared with rotary degassing.

INTRODUCTION

To address the CO₂ challenge whilst maintaining customer appeal, car manufacturers are striving towards a light-weighting solution to improve fuel economy and reduce green gas emissions. This increased interest in light-weighting materials has led to heavy investment into the advancement of high-pressure die casting (HPDC) technologies. A major defect preventing the mass production of structural components using the conventional HPDC process is gas porosity, which adversely affects the materials performance in both tensile and fatigue properties, whilst also producing blisters after subsequent heat treatment. The reduced solubility of hydrogen in liquid aluminium is believed to be a key factor influencing the nucleation and growth of gas porosity, with many novel processing techniques being developed to control the hydrogen content within the liquid metal prior to injection.

Rotary degassing is commonly used in foundries to minimise hydrogen levels in aluminium alloy melts and involves the bubbling of an inert purge gas (usually argon) into the molten metal. In this

process, a smaller purge bubble equates to a higher degassing efficiency; however it is difficult to obtain a bubble diameter below 10 mm.¹ The process therefore requires a considerably high argon flow rate between 4 L/min and 10 L/min and a significant processing time between 15 min and 30 min to achieve an acceptable hydrogen level below 0.15 cm³/100 g.² Increased rotor speeds may result in a reduced bubble size; however the increased surface turbulence and vortex introduced at these high speeds severely deteriorate the melt quality by entraining harmful oxide films.³

The degree of hydrogen supersaturation in the liquid metal depends on the hydrogen concentration, silicon concentration and melt temperature. When this supersaturation exceeds a threshold value, a gas bubble will nucleate, with the diffusion of hydrogen from the surrounding liquid resulting in the subsequent growth of bubbles.⁴ It has been suggested that the pressures required for the classical heterogeneous nucleation of gas pores are almost unattainable for aluminium alloys, prompting research into several non-classical nucleation theories. Oxide films are believed to possess the potential to nucleate gas porosity with minimal

difficulty.⁵ The diffusion of hydrogen into the air gap between the unbonded oxides causes the oxide film to unfurl, inflating to considerable size.

Previous studies on vane rheometry and direct shear cells have suggested that the rheology of equiaxed solidifying alloys can be interpreted as a cohesionless compacted granular material,^{6,7} exhibiting characteristics such as Reynolds' dilatancy (volumetric expansion in response to shear) and dilatant shear banding (regions of low crystal packing density where deformation localises). Adopting this framework, defect bands in high-pressure die casting (HPDC) are believed to form because of strain localisation in the solidifying material.^{8–11} The thicknesses of defect bands have been found to be in the range of 7–18 mean grains wide, which is in the signature range of 6–20 mean grains wide for dilatant shear banding.¹² The low crystal packing density of the band is expected to result in positive macrosegregation providing sufficient liquid can be drawn to the dilating band. When insufficient liquid is drawn into the dilating band the liquid pressure decreases, resulting in interdendritic porosity.¹¹

The Brunel Centre for Advanced Solidification Technology (BCAST) has successfully developed an alternative means of addressing these issues by the deagglomeration and dispersion of harmful oxide films and inclusions throughout the melt. This is achieved by intensive melt shearing using a rotor-stator-based high-shear-melt conditioning (HSMC) device.^{13,14} In this process, the melt is subjected to high shear rates in the gap between the rotor and stator as well as in the stator openings, resulting in effective distributive and dispersive mixing. The application of HSMC also acts to enhance nucleation by the forced wetting of oxide films and is known to reduce the size of porosity and defect bands in HPDC components.^{14,15} Degassing using the HSMC device has demonstrated improved degassing efficiency compared with rotary degassing, primarily resulting from the effective dispersion of each individual inert purge bubble into many fine bubbles, increasing the overall surface area of bubbles throughout the melt. With this process a bubble size below 1 mm can be achieved with a low argon flow rate of around 0.1 L/min.¹

A key aspect of the degassing procedure is the holding time, with an optimal value being such to allow time for the inert purge bubbles to escape through the melt surface, whilst also being sufficiently low to minimise the extent of re-gassing. The study aims to establish an optimal holding time for both rotary degassing and degassing by HSMC. The efficiency of both processing techniques will be discussed in relation to the integrity of the casting structure and the materials performance in tensile loading. The cause of failure will be analysed, with defects identified using optical microscopy and scanning electron microscopy (SEM) equipped with energy dispersive x-ray spectroscopy.

METHOD

Rheinfelden's Silafont-36 (AlSi10MnMg) HPDC aluminium alloy was used throughout this study, with measured chemical composition 9.66 wt.% Si, 0.64 wt.% Mn, 0.34 wt.% Mg, 0.096 wt.% Fe, 0.127 wt.% Ti and 0.023 wt.% Sr. Two 40-kg crucibles of Silafont-36 were melted in electric resistance furnaces and held at 750°C for 30 min to maintain a uniform composition distribution. In the first crucible, the melt was degassed using a conventional rotary degassing unit for 10 min with a stirring speed of 350 rpm and an argon flow rate of 4 L/min, in accordance with common industrial practice. The second crucible was degassed using the HSMC device, which is described elsewhere.¹ This process involved two phases (1) degassing for 10 min with a rotor speed of 1500 rpm and a considerably lower argon flow rate of 0.4 L/min followed by (2) conditioning via intensive melt shearing for an additional 20 min without argon flow. The end of gas injection marks the zero point for the subsequent holding/processing times discussed later in this article.

Following melt treatment, molten metal was poured into the shot sleeve of a Frech 4500 kN locking force cold chamber HPDC machine using a transfer ladle. The temperatures of the melt, shot sleeve and die cavity were maintained at 680°C, 180°C and 150°C respectively. The molten metal was then injected into the die cavity at a slow shot speed of 0.3 m s⁻¹ and a filling speed of 3.6 m s⁻¹ to produce eight round tensile samples with a nominal gauge diameter of ϕ 6.35 mm in accordance with ASTM standards. The geometry of the mould used to produce these tensile specimens is illustrated in Fig. 1.

After degassing, the rotary degassing unit was removed from the first crucible and the melt allowed to settle. A shot was taken every 5 min from 0 min to 25 min to observe the influence of the holding time on the performance and variability of the cast HPDC tensile specimens. After degassing by HSMC, and while the melt was subjected to intensive shearing, shots were taken every 5 min between 0 min and 25 min. The reduced pressure test (RPT) is commonly used to access the influence of hydrogen on the formation of porosity and involves solidifying the alloy in conical steel cups in air and under reduced pressure (80 mbar for 4 min).⁵ The density of the RPT samples was derived using Archimedes' principle and the density index (DI) calculated using (1), where D_{air} and D_{vac} are the density of samples solidified in air and under partial vacuum respectively.¹

$$DI = (D_{\text{air}} - D_{\text{vac}})/D_{\text{air}} \quad (1)$$

Tensile testing was carried out on an Instron 5500 universal electromechanical testing system with an extensometer gauge length of 25 mm and a cross-head speed of 1 mm/min. Tensile specimens were

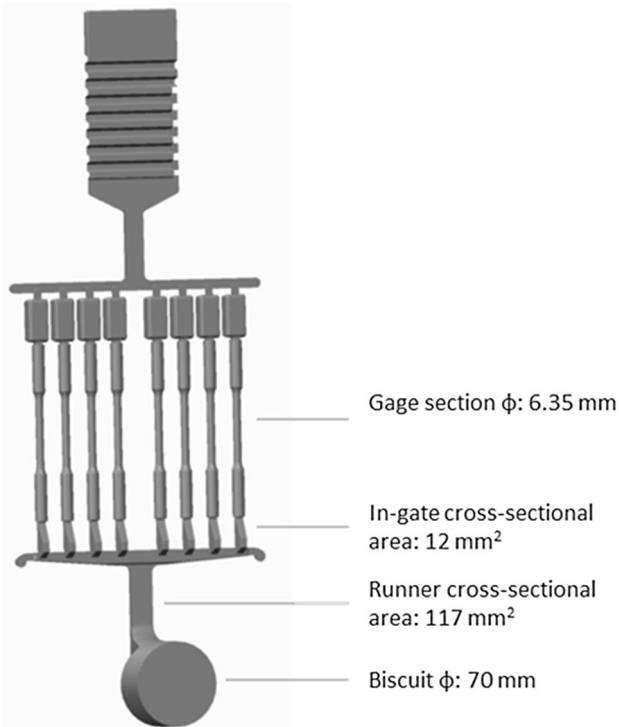


Fig. 1. Geometry of the casting used to produce tensile specimens.

aged naturally in air for 24 h and tested in the as-cast state at ambient temperature. Samples for microstructural observation were taken from the centre of the gauge length, acting perpendicular to the tensile direction. Samples were ground and polished to a 1- μm finish using standard metallographic techniques. To reveal the microstructure samples were etched with Keller's reagent (95% H_2O , 2.5% HNO_3 , 1.5% HCl , and 1% HF). The porosity levels in the HPDC cast components and from the RPT samples were observed via optical microscopy (OM) and analysed using the Fiji image-processing software package based on ImageJ.¹⁶ After tensile testing, the fracture surfaces were analysed using a tungsten filament SEM (LEO SEM 145VP; Carl Zeiss) equipped with energy-dispersive x-ray spectroscopy to identify the cause of failure in relation to the defect population.

RESULTS AND DISCUSSION

Density Index

As shown in Fig. 2, the DI values obtained from the RPT samples rapidly decrease after degassing commences, with minimum values of 2.6% and 1.0% obtained after approximately 10 min holding time for rotary degassing and 70 min for HSMC degassing respectively. These two values are well below the industrially accepted threshold of approximately 5% (0.15 $\text{cm}^3/100\text{ g}$ hydrogen). Upon reaching this minimum, the DI values are observed to

increase for samples treated with rotary degassing with increasing holding times, reaching values as high as 4.1% after 70 min. This is likely caused by the turbulence and vortex introduced during rotary degassing, which disturbs the melt surface, entraining oxide films and accelerating re-gassing of hydrogen from the newly exposed surface.³ However this increase is not observed when degassing using the HSMC device. As shown in Fig. 2, the DI values remain relatively constant, reaching a maximum of 1.4% after 190 min. This can be explained by three main mechanisms: (1) the effective dispersion of the inert purge bubbles, reducing disturbance of the melt surface previously caused by the large argon bubbles produced during rotary degassing, (2) the HSMC device is designed to produce minimal surface turbulence and vortex, decreasing the rate of re-gassing, and (3) the forced wetting of inclusions introduced by intensive shearing, removing the potency of oxide films as favourable nuclei for porosity and consequently enhancing the heterogeneous nucleation of solid during subsequent solidification processing.¹⁴ Observations of the RPT cross sections show strong agreement with the trends in DI after degassing by rotary degassing and HSMC. Porosity was found to significantly decrease after degassing commenced, subsequently increasing with increased holding times for samples treated with rotary degassing.

Mechanical Properties

Figure 3 illustrates the average yield strength (0.2% proof strength) and average elongation of four HPDC tensile samples as a function of holding time. The yield strength is shown to remain relatively stable at approximately 160 MPa for both processing techniques for the entirety of the experiment. This value of 160 MPa is higher than the yield strength of 141 MPa quoted by Rheinfelden for a Mg content of 0.33 wt%.¹⁷ The variability in elongation for the HPDC cast tensile specimens is shown to also reach a minimum at 10-min holding time, corresponding to the DI values obtained in Fig. 2. Dybalska et al.¹⁸ established an optimal mixing time of 4 min for 2.7 dm^3 of liquid aluminium for effective liquid metal processing. Once linearly scaled for a 40-kg crucible and a rotor speed of 1500 rpm, an optimal mixing time of approximately 44 min is predicted. This corresponds very well with the results obtained in this experiment. With increasing holding time, the variation for both processing techniques also increases. For rotary degassing this is likely caused by the previously mentioned re-gassing mechanisms. However, the observed increase in variation at later HSMC holding times is unexpected and may result from disturbance of the surface introduced whilst collecting samples or from the formation of other underlying defects during the HPDC process.

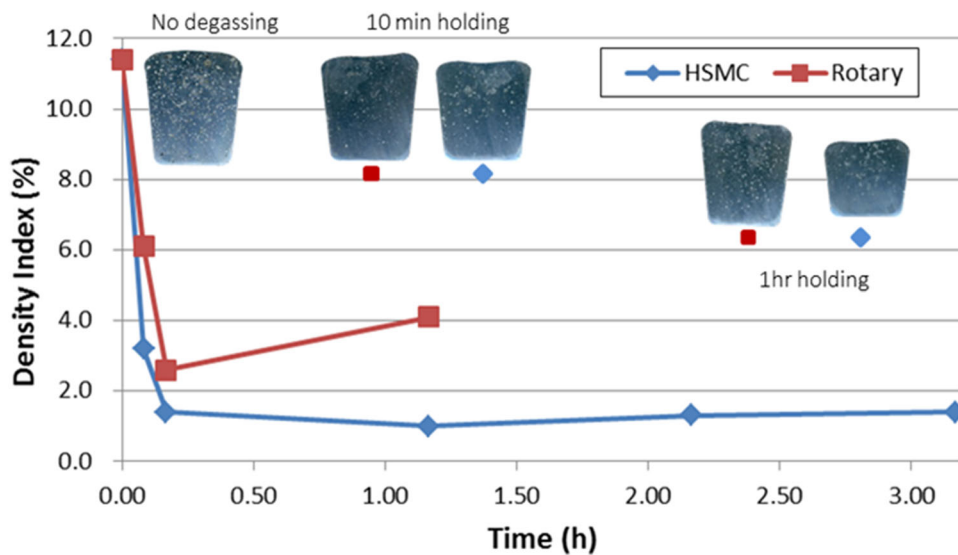


Fig. 2. The effect of holding time on the density index of RPT samples.

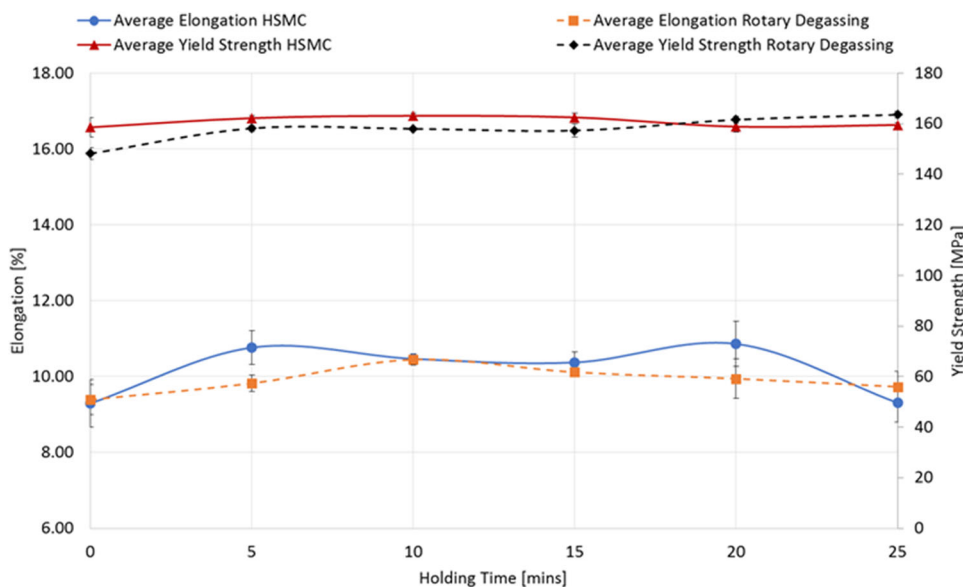


Fig. 3. Average elongation, average yield strength and variability of tensile performance as a function of holding time.

Porosity Distribution and Defect Bands

The HPDC samples for both processing techniques exhibited considerable porosity, particularly towards the centre of the casting (Fig. 4). After degassing, gas porosity was significantly reduced; however macropores resulting from solidification shrinkage remained. Defect bands of positive macrosegregation were observed in both samples treated with rotary degassing and HSMC, located towards the centre of the casting and following the casting contour. As shown in Fig. 4, samples treated with HSMC exhibit a reduced defect band thickness compared with those treated with rotary degassing. This has been attributed to the uniform distribution of externally solidified crystals after the application

of intensive melt shearing, which in turn influences the mush rheology during filling and subsequent feeding of the casting.^{11,14}

Optical micrographs taken at higher magnification from the centre of the cross section were used to determine the gas pore density and average pore size as shown in Table I and Fig. 5. Within the Fiji image processing software package based on ImageJ, optical micrographs were binarised using an appropriate threshold to differentiate pores from the matrix, as shown in Fig. 5. Pores with circularity above 0.5 were classified as gas porosity and separated for further analysis (the number of these gas pores is denoted N_p). The average pore size (Φ) was determined using the equivalent circle

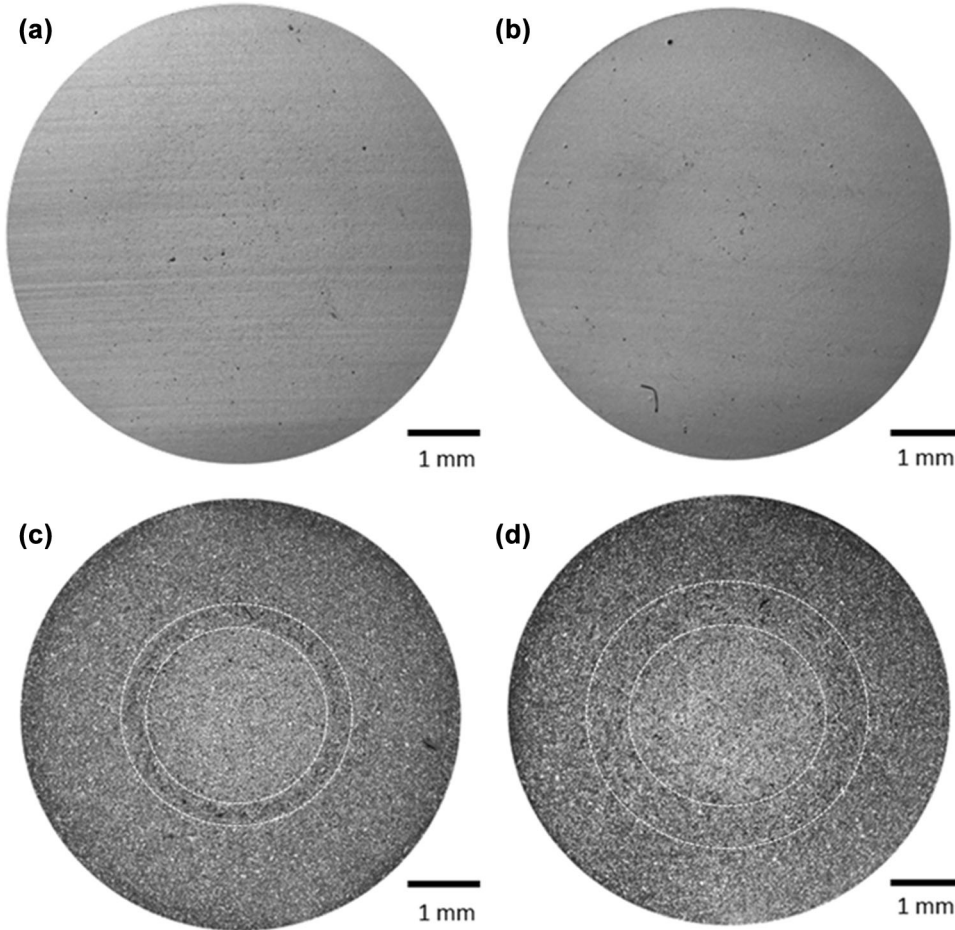


Fig. 4. Pore distribution (a, b) and defect bands (c, d) of samples taken from the gauge length perpendicular to the tensile direction. Showing HPDC specimens treated with HSMC (left) and rotary degassing (right) for a holding time of 10 min.

Table I. Comparison between pore density and pore size for castings treated with HSMC and rotary degassing at holding times of 0 min, 10 min and 30 min

	0 min after degassing		10 min after degassing		30 min after degassing	
	Pore density N_p/mm^2	Pore Φ μm	Pore density N_p/mm^2	Pore Φ μm	Pore density N_p/mm^2	Pore Φ μm
HSMC degassing	434 ± 4	3.1 ± 0.8	495 ± 4	4.8 ± 0.3	436 ± 14	3.8 ± 0.4
Rotary degassing	205 ± 24	4.3 ± 0.3	230 ± 19	5.1 ± 1.7	341 ± 66	5.3 ± 0.4

All values were calculated using Fiji (ImageJ) using optical micrographs shown in Fig. 5.

approach, using (2), and the pore density was defined as the number of pores in the image divided by the image area.

$$\text{Area of pore} = \frac{\pi\phi_i}{4}, \phi = \sum \frac{\phi_i}{N_p} \quad (2)$$

Samples treated with HSMC exhibit a decreased pore size and increased pore density compared with those treated with rotary degassing. This is caused

by the effective dispersion of the argon purge bubbles during HSMC, leading to a high density of fine pores using a substantially reduced argon flow rate compared with rotary degassing. For samples treated with rotary degassing, the increased pore size at 10 min holding time appears to contradict the DI values observed in Fig. 2. Although the hydrogen content might be at a minimum, the melt turbulence introduced during rotary degassing entrains oxide films from the surface, providing an initiation source

for porosity.¹⁹ Whilst increased holding times provide sufficient time for the evacuation of hydrogen through the surface, when the melt quality is poor sufficient time is also provided for the diffusion of hydrogen into the bifilm, causing it to unfurl. For HSMC, the forced wetting of oxide films removes their potency as nuclei for gas porosity; therefore the sudden increase in porosity after 10 min shearing is unexpected and likely results from the disturbance of the melt surface during collection of the samples.

Fracture Analysis

Observation of fracture surfaces via SEM equipped with energy-dispersive x-ray spectroscopy was carried out to identify defects relating to

fracture. For the samples treated with HSMC at 10-min processing time, defects observed within the fracture path mainly constituted large Fe-rich intermetallic particles and smaller cubic-shaped Mn-rich intermetallic particles (Fig. 6). For the samples treated with rotary degassing, along with the Mn-rich intermetallic particles previously mentioned, a large oxide film was also observed towards the casting surface (Fig. 7). These large oxides were likely entrained during rotary degassing and were not found in the HSMC-treated samples because of the effective deagglomeration of oxide films with the application of intensive melt shearing.¹⁴ The presence of these large oxide films will have a significant impact on the variability of mechanical properties, particularly elongation.

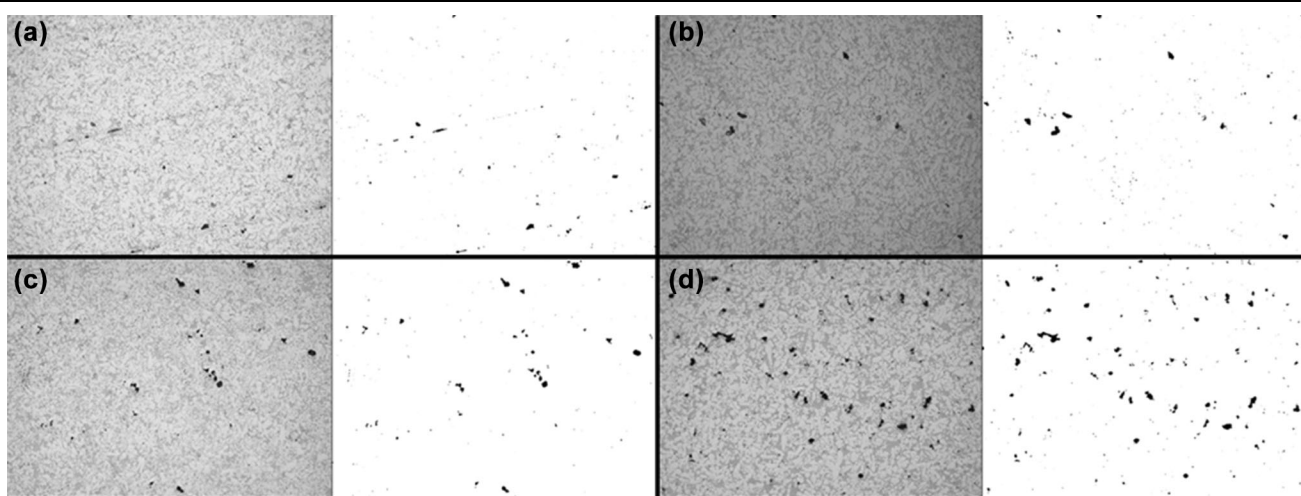


Fig. 5. Optical micrographs and corresponding binarised images taken from the centre of the HPDC samples used to quantify the pore density and size for samples treated with HSMC for (a) 0 min holding and (b) 30 min holding and samples treated with rotary degassing for (c) 0 min holding (d) 30 min holding.

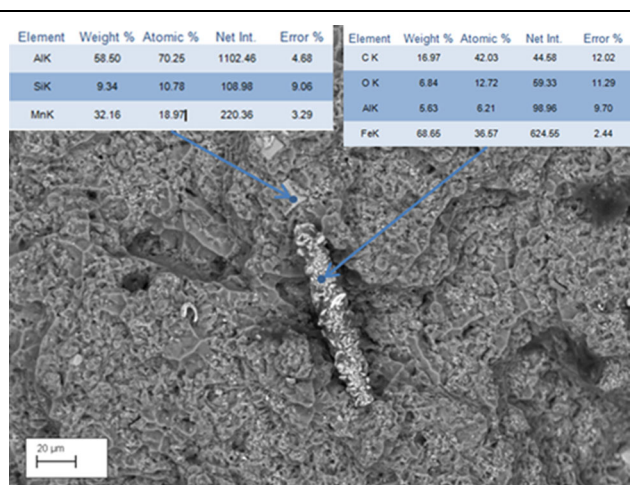


Fig. 6. SEM micrograph showing Fe-rich and Mn-rich intermetallic particle compounds on the fracture surface of an HPDC tensile specimen treated with HSMC for 10 min holding. Values from the energy-dispersive x-ray spectrum are shown in the tables.

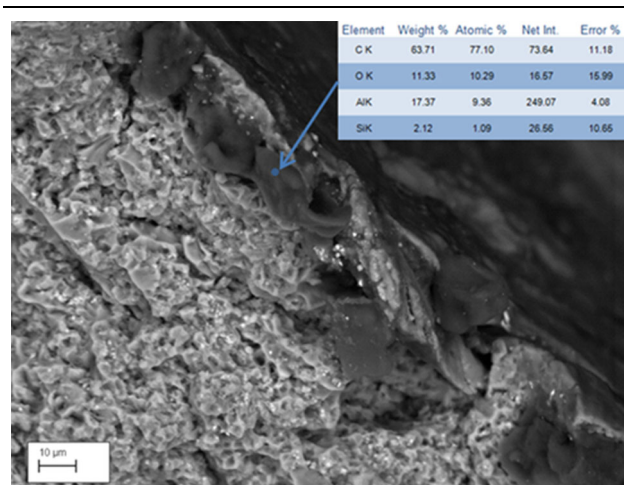


Fig. 7. SEM micrograph showing an oxide film on the fracture surface of an HPDC tensile specimen treated with rotary degassing for 10 min holding. Values from the energy-dispersive x-ray spectrum are shown in the table.

CONCLUSION

Two 40-kg melts of Silafont-36 HPDC aluminium alloy were degassed using rotary degassing and HSMC respectively, with tensile samples produced using the cold-chamber HPDC process. For both melt treatments, an optimal holding time of 10 min was established corresponding to minimum hydrogen content and minimum variation in the tensile performance of the HPDC cast specimens. Upon reaching this minimum, the DI and tensile variation increases for the melt treated with rotary degassing, believed to be caused by the surface turbulence and vortex introduced during processing. For samples treated with HSMC, the variation increases with increasing holding time; however the DI values remain in a quasi-steady state. This increase in variation was linked to disturbance of the melt surface during sample collection and the formation of casting defects such as the Fe- and Mn-rich intermetallic particles observed with SEM. Optical microscopy revealed that the samples conditioned using the HSMC device contained smaller pores and a higher pore density compared with those treated with rotary degassing, despite the use of a considerably lower argon flow rate of 0.4 L/min. The increased degassing efficiency observed for the HSMC device results from the effective dispersion of the large inert purge bubbles leading to many fine pores. For rotary degassing, the pore size and density were found to increase with prolonged holding times, corresponding to the increased DI values and the variation in tensile performance. For the samples treated with rotary degassing, a large oxide film was observed near to the casting surface, which is likely to have been introduced during degassing. For the HPDC samples treated with HSMC no oxide films were observed.

ACKNOWLEDGEMENTS

The authors acknowledge the financial support provided by the Engineering and Physical Sciences Research Council (EPSRC). The authors sincerely thank Dr. Kun Dou for producing simulations aiding in the research.

REFERENCES

1. J.B. Patel, J.L. Nebreda, and Z. Fan, in *Proceedings of 6th Decenn. International Conference on Solidification Processing* (Old Windsor, 2017).
2. J. Davis, *ASM Int.* 3, 784 (1993).
3. D. Dispinar, S. Akhtar, A. Nordmark, M. Di Sabatino, and L. Arnberg, *Mater. Sci. Eng. A* 527, 3719 (2010).
4. R.C. Atwood and P.D. Lee, *Metall. Mater. Trans. B* 33, 209 (2002).
5. D. Dispinar and J. Campbell, *Int. J. Cast Met. Res.* 17, 280 (2004).
6. A.K. Dahle and D.H. StJohn, *Acta Mater.* 47, 31 (1998).
7. C.M. Gourlay, B. Meylan, and A.K. Dahle, *Acta Mater.* 56, 3403 (2008).
8. A.K. Dahle, S. Sannes, D.H. St. John, and H. Westengen, *J. Light Met.* 1, 99 (2001).
9. C.M. Gourlay and A.K. Dahle, *Nature* 445, 70 (2007).
10. C.M. Gourlay, H.I. Laukli, and A.K. Dahle, *Metall. Mater. Trans. A Phys. Metall. Mater. Sci.* 35, 2881 (2004).
11. C.M. Gourlay, H.I. Laukli, and A.K. Dahle, *Metall. Mater. Trans. A Phys. Metall. Mater. Sci.* 38, 1833 (2007).
12. S. Otarawanna, C.M. Gourlay, H.I. Laukli, and A.K. Dahle, *Mater. Charact.* 60, 1432 (2009).
13. Z.Y. Fan, Y.B. Zuo, and B. Jiang, *Mater. Sci. Forum* 690, 141 (2011).
14. H.R. Kotadia, N. Hari Babu, H. Zhang, S. Arumuganathar, and Z. Fan, *Metall. Mater. Trans. A Phys. Metall. Mater. Sci.* 42, 1117 (2011).
15. J.B. Patel, X. Yang, C.L. Mendis, and Z. Fan, *JOM* 69, 1071 (2017).
16. Fiji/ImageJ, <https://imagej.nih.gov/ij/>. Last accessed 23 Aug 18.
17. Rheinhfelden, CAR DS-Mould Des. 1 (2015).
18. A. Dybalska, D. Eskin, and J.B. Patel, *JOM* 69, 720 (2017).
19. J. Campbell, *Castings*, 2nd ed. (Oxford: Butterworth-Heinemann, 2003).